

Neutron background at the Canfranc Underground Laboratory and its contribution to the IGEX-DM dark matter experiment

J.M. Carmona, S. Cebrián, E. García, I.G. Irastorza, G. Luzón, A. Morales*, J. Morales, A. Ortiz de Solórzano, J. Puimedón, M.L. Sarsa, J.A. Villar.

Laboratory of Nuclear and High Energy Physics, University of Zaragoza, 50009 Zaragoza, Spain

Abstract

A quantitative study of the neutron environment in the Canfranc Underground Laboratory has been performed. The analysis is based on a complete set of simulations and, particularly, it is focused on the IGEX-DM dark matter experiment. The simulations are compared to the IGEX-DM low energy data obtained with different shielding conditions. The results of the study allow us to conclude, with respect to the IGEX-DM background, that the main neutron population, coming from radioactivity from the surrounding rock, is practically eliminated after the implementation of a suitable neutron shielding. The remaining neutron background (muon-induced neutrons in the shielding and in the rock) is substantially below the present background level thanks to the muon veto system. In addition, the present analysis gives us a further insight on the effect of neutrons in other current and future experiments at the Canfranc Underground Laboratory. The comparison of simulations with the body of data available has allowed to set the flux of neutrons from radioactivity of the Canfranc rock, $(3.82 \pm 0.44) \times 10^{-6} \text{ cm}^{-2} \text{ s}^{-1}$, as well as the flux of muon-induced neutrons in the rock, $(1.73 \pm 0.22(\text{stat}) \pm 0.69(\text{syst})) \times 10^{-9} \text{ cm}^{-2} \text{ s}^{-1}$, or the rate of neutron production by muons in the lead shielding, $(4.8 \pm 0.6(\text{stat}) \pm 1.9(\text{syst})) \times 10^{-9} \text{ cm}^{-3} \text{ s}^{-1}$.

Key words: Underground muons, dark matter, muon flux, neutron background
PACS: 28.20.Gd, 96.40.Tv, 25.30.Mr, 95.35.+d

The search for dark matter is one of the biggest challenges of modern cosmology. Last observational data [1,2,3] are compatible with a flat accelerating

* Deceased.

Universe with a matter content of around 30%, where about 25% is dark matter, mostly in the form of non-baryonic cold dark matter. Even though the Standard Model (SM) of particle physics does not offer a proper candidate satisfying all the needed requirements, its supersymmetric extensions open a new world of particles. Experiments looking for cold, non-baryonic, weakly interacting, massive neutral particles beyond the SM —generically called WIMPs— supposedly forming this missing matter of the Universe are obviously of most relevance for particle physics and cosmology and so the number of such attempts —with a large variety of techniques, detectors and targets— is quite numerous [4].

In experiments intended for WIMP direct detection, such as IGEX Dark Matter (IGEX-DM), galactic WIMPs could be detected by means of the nuclear recoil they would produce when scattered off target nuclei of suitable detectors. The sensitivity of these experiments has been continuously increasing since the first searches, more than fifteen years ago, thanks to higher levels of radiopurity of detectors, discrimination techniques and a deeper understanding of the various sources of radioactive background. The study of the background of these experiments is then a very important activity in their development. Even though the neutron component of the background has been always a matter of concern for shallow site experiments [5], in deep underground locations it used to be by far below the level of the typical gamma background. More recently, however, the extreme level of radiopurity and the expertise achieved in low background techniques, as in the case of IGEX [6,7,8], has reduced the raw background to levels where the neutron contribution can be of great importance. These facts, together with the recent development of discrimination techniques to disentangle nuclear recoils produced by particle dark matter interactions from electron recoils generated by the typical gamma or beta background [9,10,11,12] have made the neutrons to remain as the real worrisome background for WIMPs [13,14,15,16]. They can produce nuclear recoils (< 100 keV) in the detector target nuclei which would mimic WIMP interactions. Simple kinematics tells that in the case of germanium, neutrons of 1(5) MeV could elastically scatter off germanium nuclei producing recoils of energies up to 54(268) keV.

The present work deals with the study of the neutron background in the underground environment of the Canfranc Underground Laboratory (LSC) (2450 m.w.e., see Fig. 1), and in particular of its fast component with effect on the IGEX-DM experiment. In Section 1 the IGEX-DM experiment is briefly described, especially in the aspects relevant to the present analysis, such as, for instance, the lead and polyethylene shieldings and the active veto system. The body of data available for this study is also presented. In Section 2, a brief outline of the simulations performed and their technical details are given. Sections 3, 4 and 5 present the results from the simulations and their comparison with experimental data concerning the three relevant neutron populations.

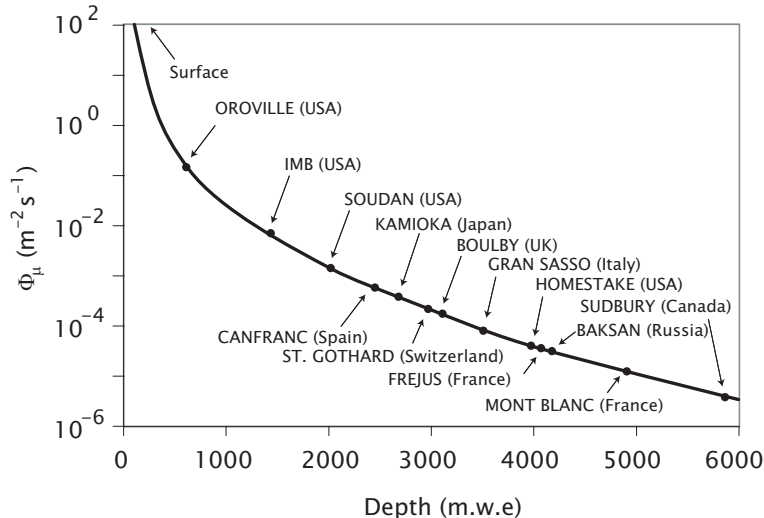


Fig. 1. Dependence of muon flux with depth, showing the location of the Canfranc Underground Laboratory with respect to other underground facilities.

The final conclusions are gathered in Section 6.

1 The IGEX Dark Matter Experiment

The IGEX experiment, originally optimized for detecting ^{76}Ge double beta decay, has been described in detail elsewhere [17]. One of the enriched (86% in ^{76}Ge) IGEX detectors (named RG-II) of 2.2 kg (2.0 kg active mass) is being used to look for WIMPs interacting coherently with the germanium nuclei. Its full-width at half-maximum (FWHM) energy resolution is 2.37 keV at the 1333 keV line of ^{60}Co , and the low energy long-term energy resolution (FWHM) is 1 keV at the 46.5 keV line of ^{210}Pb . The lines of an external ^{22}Na source and the excited X-rays of Pb have been used for periodic energy calibrations at high and low energies.

We refer to papers [6,7,8] where the latest results of the experiment regarding dark matter searches are presented and where the aspects related to the experimental set-up, shielding, data acquisition system, etc. are described. The threshold of the experiment is 4 keV and the raw background registered in the region just above the threshold is of a few tenths of counts/(kg day keV), the lowest raw background (i.e. with no nuclear recoil discrimination mechanism) ever achieved in this energy range.

Particularly interesting for the purpose of the present work is the shielding used in the experiment. Leaving more detailed information for the references previously mentioned, it can be described as follows. The innermost part consists of about 2.5 tons of 2000-year-old archaeological lead (having < 9 mBq/kg

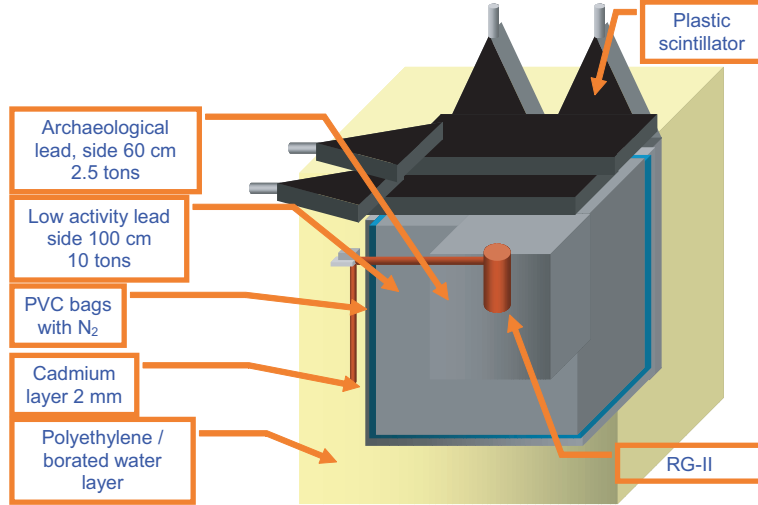


Fig. 2. Sketch of the experimental set-up. Four more vetoes, covering two lateral sides of the cube, have been removed for better visualization of the figure.

of ^{210}Pb (^{210}Bi), $< 0.2 \text{ mBq/kg}$ of ^{238}U , and $< 0.3 \text{ mBq/kg}$ of ^{232}Th) forming a cubic block of 60 cm side. The germanium detector is fitted into a precision-machined chamber made in this central core, which minimizes the empty space around the detector available to radon. Nitrogen gas, at a rate of 140 l/hour, evaporating from liquid nitrogen, is forced into the small space left in the detector chamber to create a positive pressure and further minimize radon intrusion. The archaeological lead block is surrounded by 20 cm of lead bricks made from 70-year-old low-activity lead (~ 10 tons) having $\sim 30 \text{ Bq/kg}$ of ^{210}Pb . The whole lead shielding forms a 1 m side cube, the detector being surrounded by not less than 40-45 cm of lead (25 cm of which is archaeological). Two layers of plastic seal this central assembly against radon intrusion and a 2-mm-thick cadmium sheet surrounds the ensemble. Specially relevant for the present work are the cosmic muon vetoes (BC408 plastic scintillators) covering the top and three sides of the shield. Its effect on the background reduction in the low energy region will be stressed in Section 3, where the neutrons induced by muons in the shielding are studied. Finally, an external neutron moderator (made of polyethylene bricks and borated water tanks) surrounds the whole set-up. Its thickness has been changed in several occasions, giving rise to independent sets of data whose differences will be particularly useful in this analysis. See a sketch of the set-up in Fig. 2.

The body of data to be used in the present work has been divided in four different sets (A, B, C and D) according basically to the thickness of the outer neutron moderator wall used in the shielding (0, 20, 40 and 80 cm respectively). Some parameters concerning each set of data are quoted in Table 1, and the low energy spectral shapes are plotted in Fig. 3. The sets B and C correspond mostly to the data already presented in Refs. [6] and [7] respectively with added statistics. The data sets A and D were taken more recently to complete

the present analysis. A word of caution must be said concerning the oldest data set B since there are more differences in the experimental set-up with respect to the other sets than just the neutron shielding: four Ge detectors were in the same lead shielding and the outer location of the corresponding four liquid N₂ dewars left two of the shielding sides without moderator. Therefore, set B will be included in some plots just to have another intermediate situation between the two extreme cases A and D, but no quantitative conclusion about neutrons will be drawn from it. In the other three data sets (A, C and D) the experimental set-up has been exactly the same except for the thickness of the moderator wall.

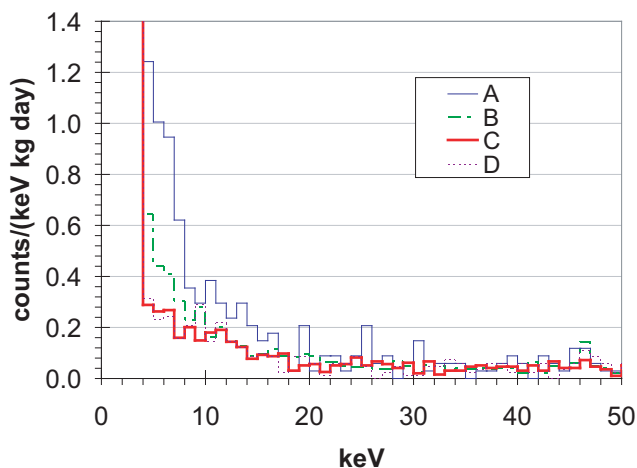


Fig. 3. Low energy region of the measured spectra for each set of data, having a different thickness of neutron moderator: A, 0 cm; B, 20 cm; C, 40 cm and D, 80 cm.

Table 1

Main features of the data sets A, B, C and D: statistics time, thickness of the neutron moderator and measured average background level (in anticoincidence with the veto system) from 4 to 10 keV.

	A	B	C	D
thickness of moderator (cm)	0	20	40	80
statistics time (days)	17	118	97	41
background [counts/(kg keV day)]	0.74(6)	0.39(2)	0.22(1)	0.24(2)

The differences of the spectra shown in Fig. 3 appear to be consistent with the corresponding thicknesses of the neutron moderator wall used. The thicker the wall, the lower the background, excepting the last step from 40 to 80 cm which basically does not improve it further. The successive reduction from the first batch of IGEX-DM data [6] was tentatively interpreted as due to the disappearance of neutrons after the increase of the neutron moderator thickness [7]. This interpretation is confirmed in the present work, where a

general and quantitative study of the effect of neutrons on IGEX-DM has been performed.

2 General outline of the simulations performed

In deep underground locations neutrons have two possible origins: either they are produced by natural radioactivity in the material surrounding the detector or they are induced by muons, the only cosmic component still present there. The relevant muon-induced neutrons are produced in the last few meters of rock surrounding the laboratory or in the lead shielding itself, the difference being extremely important, because the latter can be rejected by the muon veto system while most of the former cannot. Therefore, three different populations of neutrons have been simulated: muon-induced neutrons in the shielding itself, muon-induced neutrons in the surrounding rock and neutrons from radioactivity in the rock. The description of the simulation in each case and the corresponding results will be presented independently in the following sections.

In underground locations such as the LSC (2450 m.w.e.), where the flux of cosmic muons has been notably suppressed, the neutrons from radioactivity in the rock are usually dominant in comparison with the muon-induced neutrons [18]. However, because of the energies of the neutrons from radioactivity (< 10 MeV) they can be more easily and effectively shielded than those originated by muons (whose energies go up to several hundreds of MeV). More quantitative discussions are left for the following sections.

Neutrons produced by radioactivity in the shielding materials have not been included in the simulations since, owing to the extreme radiopurity of such materials, its contribution has been estimated to stand three orders of magnitude below the present level of background.

Two different kinds of simulations have been performed. The first one is that of the transport and interaction of the different populations of neutrons through the IGEX geometry. These simulations have been performed with the GEANT4 code [19] using the high precision neutron data library G4NDL3.5. The incoming neutrons have been launched isotropically and uniformly, either from the outer surface of the shielding in the case of neutrons from the rock or from the whole lead volume in the case of neutrons induced in the shielding. Spectral samplings are described and justified later. The spectra shown as a result of these simulations correspond always to the energy depositions of the neutrons in the active volume of the germanium detector (nuclear recoils) corrected for a quenching factor of 0.25 in Ge, so that they can be directly compared with the experimental data shown always in electron-equivalent en-

ergy. On the other hand, some complementary simulations to study the neutron production by muons in several generic situations have been performed with the FLUKA code [20], of proven reliability when hadronic processes are involved. These simulations provide the neutron spectrum exiting a layer of material when a known flux of muons traverses it, as well as the total neutron yield. We note that in our simulation results we will not consider systematic errors coming from the specific implementation of physical processes by these Monte Carlo codes.

3 Muon-induced neutrons in the shielding

The production of neutrons by muons interacting in matter is not a simple subject, many different processes coming into play. The total neutron flux and spectral shape depend on the target material as well as on the muon energy, and therefore on the depth. Following the practical approach of Refs. [16,21] we distinguish two different sets of muon-induced neutrons, according to their typical energies: high energy (HE) neutrons going up to several hundreds of MeV which are produced basically by hadron showers originated by the muons, and medium energy (ME) going up only to 20-30 MeV, produced by photonuclear reactions related to electromagnetic showers, capture of slow muons (of very little importance at deep places), elastic interaction of muons with neutrons inside nuclei and secondary neutrons produced after one of the previous processes. Even though neutrons are produced in any shielding material we will focus on those originated in lead owing to its higher neutron yield and to its closeness to the detector. In order to determine their spectral shape we have simulated with the FLUKA code the outcome of muons passing through lead. The energy spectrum of muons corresponding to the 2.5 km.w.e. depth of the LSC has been sampled following Ref. [22].

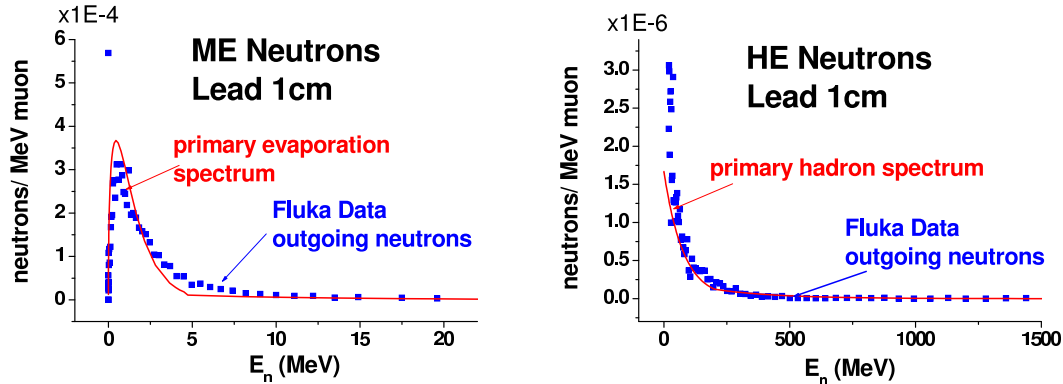


Fig. 4. Energy spectrum of muon-induced neutrons in lead according to the FLUKA simulation (squares) compared to the analytical approximations used for ME and HE (solid lines).

In Fig. 4 the result of such simulation for 1 cm of lead is shown for both ME and HE populations. Such a small thickness avoids the production of secondary neutrons and spectral deformations due to neutron transport through the lead slab. The obtained spectra, which are therefore the production spectra for primary neutrons, turns out to be in satisfactory agreement with the analytical approximation proposed in [5] for ME neutrons in lead,

$$\frac{dN}{dE} = \begin{cases} 0.812 E^{5/11} \exp(-E/1.22) & \text{for } E < 4.5 \text{ MeV} \\ 0.018 \exp(-E/9) & \text{for } E > 4.5 \text{ MeV} \end{cases} \quad (1)$$

and, in the case of HE neutrons, with the analytical formula

$$\frac{dN}{dE} = \begin{cases} 6.05 \exp(-E/77) & \text{for } E < 200 \text{ MeV} \\ \exp(-E/250) & \text{for } E > 200 \text{ MeV} \end{cases} \quad (2)$$

which was originally proposed in [16,21] for describing the HE neutron spectrum in rock. In these formulas E is the emitted neutron energy (in MeV).

This simulation underestimates the total neutron yield since showers, main sources of secondary neutrons, do not develop in 1 cm of lead. The neutron yield obtained after 1 cm of lead, $8.8 \times 10^{-5} (\text{g/cm}^2)^{-1}$ per muon, including only primary neutrons, agrees with the numbers presented in [14,15] for neutrons produced in inelastic processes. The total neutron yield including also secondary neutrons can be estimated by a second simulation with a thicker lead layer (35 cm). The obtained number, $1.7 \times 10^{-3} (\text{g/cm}^2)^{-1}$ neutrons per muon, is pretty close to the value estimated in [13] for the total neutron yield. Therefore, secondary neutrons coming from showers dominate the muon-induced neutron population. These secondary neutrons follow mainly the evaporative spectrum described by Eq. (1) while primary spallation neutrons can be sampled by Eq. (2).

Simulations of neutrons isotropically distributed in the full lead volume of the IGEX geometry with spectra given by Eqs. (1) and (2) were performed using GEANT4. The resulting spectra at the detector turn out to be essentially independent of the relative weight of ME neutrons and HE neutrons, and is shown in Fig. 5. The difference between the energy distributions produced using these two spectra (HE and ME) is small enough to make the relative abundance of HE and ME neutrons in the input spectrum not crucial for our purposes.

Let us compare now these neutron simulations with experimental data. As stated before, background events coming from muon-induced neutrons in the shielding can be rejected by the muon veto system. The rejected events are those appearing in the experimental coincidence spectrum between detec-

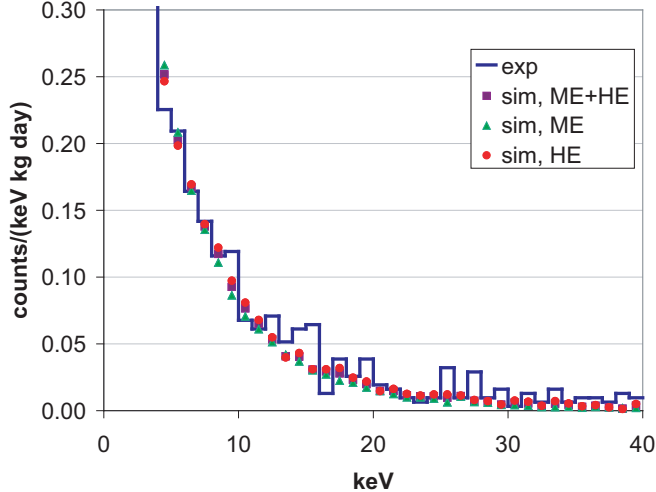


Fig. 5. Comparison of the measured spectrum of vetoed events (labelled *exp*) with the simulated spectra of electron-equivalent energy deposited in the detector by muon-induced neutrons in lead, assuming the HE spectrum, the ME spectrum and a weighted combination (50% ME, 50% HE).

tor and vetoes. This can be compared with the simulation results to get the normalization of muon-induced neutrons in the IGEX shielding, assuming that no other kind of events different from muon-induced neutrons are present in the coincidence spectrum. We have checked that random coincidences and events produced by direct interaction of muons in the detector are at least 2 orders of magnitude below the total rate of the coincidence spectrum [0.16 counts/(keV kg day) in 4-10 keV], so that it can be safely compared with the simulation. This experimental spectrum is independent of the thickness of the polyethylene wall. In Fig. 5, the normalization of the spectrum produced by the simulation has been adjusted to fit the experimental data. From that fit the neutron production by muons in the IGEX lead can be deduced to be $(4.8 \pm 0.6(stat) \pm 1.9(syst)) \times 10^{-9} \text{ cm}^{-3} \text{ s}^{-1}$. The systematic error accounts only for the unknown fraction of HE and ME neutrons and it has been estimated by calculating the neutron production in the extremal cases of all neutrons having either the HE or the ME spectrum. Taking into consideration the effect of the evaluated rates of vetoed events which do not correspond to neutrons, the corresponding error is estimated to be of 0.4%; this systematic error is negligible with respect to that due to the unknown fraction of HE and ME neutrons. Using the total neutron yield previously obtained by the muon simulation together with the estimated neutron production, the total muon flux crossing the shielding can be estimated and the known errors propagated, giving $(2.47 \pm 0.31(stat) \pm 0.98(syst)) \times 10^{-7} \text{ cm}^{-2} \text{ s}^{-1}$.

The obtained muon flux is of the expected order of magnitude at 2450 m.w.e., and in fact it is in perfect agreement with previous scintillator measurements at the LSC site, which gave a flux of $2 \times 10^{-7} \text{ cm}^{-2} \text{ s}^{-1}$ [7], therefore showing

the reliability of our numerical simulations.

It is worth noting that the contribution of the muon-induced neutrons generated in the shielding to the background levels is not negligible, but thanks to the veto system it is significantly reduced. The veto counting rate, shown in Fig. 5, in the low energy region (4-10 keV) in IGEX-DM is 0.16 counts/(keV kg day). For a veto efficiency ϵ , such a rate would imply a background contribution of $0.16 \times (1 - \epsilon)/\epsilon$ counts/(keV kg day). The efficiency of the veto system is estimated to be well above 92% so that the contribution of these neutrons is less than 1.3×10^{-2} counts/(keV kg day). This value is more than one order of magnitude lower than the present background level, but it might become an important contribution in future experiments. GEDEON (GERmanium DETectors in ONe cryostat) is a new project on WIMP detection using larger masses of germanium of natural isotopic abundance [4]. It will use the technology developed for the IGEX experiment and consist of a set of ~ 1 kg germanium crystals (total mass of about 28 kg), placed together in a compact structure inside one only cryostat. This approach could benefit from the anti-coincidence between the crystals and a lower components/detector mass ratio to further reduce the background with respect to IGEX. In this project a more efficient veto system should be designed to minimize the contribution of the neutrons induced by muons in the shielding.

4 Muon-induced neutrons in the surrounding rock

Neutrons produced by muons in the last few meters of the underground laboratory rock are much less abundant than neutrons coming from radioactivity. However, they could be relevant because of their much higher energies. In addition, most of the muon-induced neutrons in the rock are not detected by the veto system and become as important as neutrons induced in the shielding itself, even though these are produced much closer to the detector. Following similar steps to those of the previous section, we have first studied the neutron outcome after the muons have traversed the overburden rock. We have performed a FLUKA simulation with a muon spectrum corresponding to 2450 m.w.e. traversing a layer of rock thick enough (10 meters) since neutrons produced farther inside the rock would never reach laboratory walls. The total neutron yield is 4.6×10^{-4} (g/cm²)⁻¹ per muon, compatible with values shown in other references [14,15,23].

The relevant parameter we are interested in is, however, the outgoing neutron outcome. In Fig. 6 we represent both outgoing neutrons populations, HE and ME. We will no longer be concerned about ME neutrons (0.01 neutrons per muon) since, like those more abundant coming from radioactivity, they are easily shielded as we will show in the next section. Therefore we will just

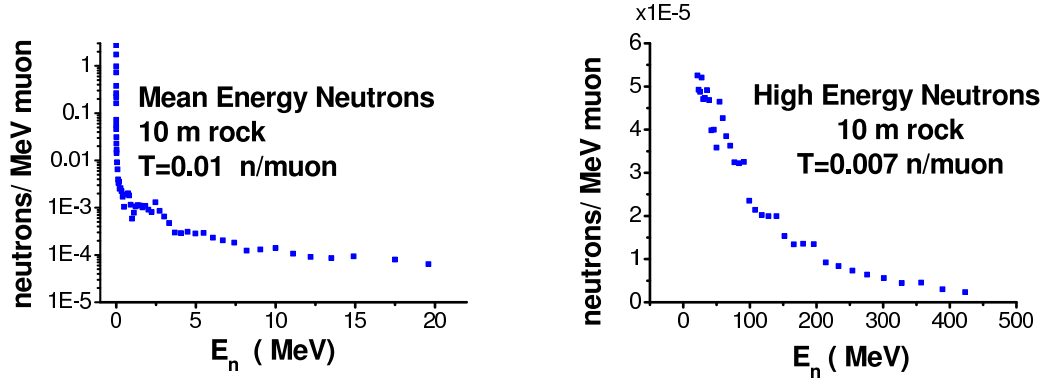


Fig. 6. Energy spectrum of outgoing muon-induced neutrons in rock according to the FLUKA simulation (squares).

focus on HE (> 20 MeV) outgoing neutrons whose yield results in a lower value of 0.007 neutrons per muon. This allows to compute the total muon-induced neutron flux coming out of the rock using the muon flux of the previous section. The estimated result is $(1.73 \pm 0.22(stat) \pm 0.69(syst)) \times 10^{-9} \text{ cm}^{-2} \text{ s}^{-1}$.

High-energy neutrons with the spectral shape of Fig. 6 [which follows the analytical form of Eq. (2)] have been launched from the outer shielding surface for the different thicknesses of moderator of sets A–D to simulate their transportation and interaction through the IGEX geometry. The results of these simulations are shown in Fig. 7 and the integrated values in Table 2.

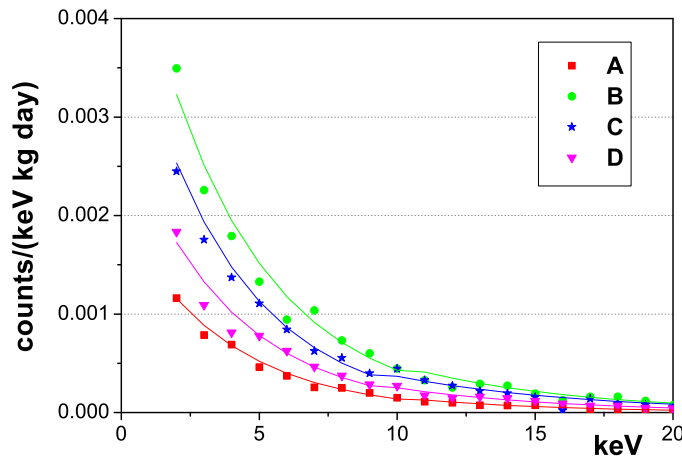


Fig. 7. Energy spectra deposited in the detector by muon-induced neutrons in rock at a depth of 2450 m.w.e.: simulation for the different set-ups. Fits to exponential curves have been drawn to guide the eye.

It is interesting to see that the contribution is maximum for the intermediate value of 20 cm of neutron moderator, decreasing for thicker walls or in the case of total absence of polyethylene: very energetic neutrons (with some hun-

Table 2

Simulated background rates in IGEX-DM for the energy region from 4 to 10 keV due to μ -induced neutrons in the rock for the different set-ups for a neutron flux of $1.73 \times 10^{-9} \text{ cm}^{-2} \text{ s}^{-1}$. Only statistical errors are quoted.

	counts/(keV kg day)
A	0.00041(1)
B	0.00124(4)
C	0.00091(4)
D	0.00061(3)

dreds of MeV), which produce nuclear recoils corresponding mostly to energies higher than our range of interest in the absence of moderator walls, can be slowed down in the presence of the polyethylene shielding, inducing in this way nuclear recoils in the low-energy region. In any case, the contribution of these neutrons to the IGEX-DM background is much lower than the present background level.

5 Neutrons from radioactivity in the surrounding rock

Neutrons can be produced in the rock by spontaneous fission of uranium and (α , n) reactions. The intensity of the corresponding outgoing neutron flux is therefore dependent on the kind of rock. In fact, several estimates of this flux in deep underground locations give values in a range from 10^{-6} to $10^{-5} \text{ cm}^{-2} \text{ s}^{-1}$ [13,16,18,24,25,26,27,28,29,30]. To sample the incident energies of fission neutrons a typical fission spectrum has been used (energy E is expressed in MeV):

$$\frac{dN}{dE} \propto E^{1/2} \exp(-E/1.29) \quad (3)$$

while the spectral sampling for neutrons from (α , n) reactions is performed following the calculated spectrum shown in Fig. 11 of Ref. [27], deduced for the Modane Laboratory. These spectra can be used to sample the incident energies since the spectrum does not suffer any significant deformation after the neutrons have traversed several meters of rock. Although the neutron spectrum coming from (α , n) processes is expected to be dependent on the type of rock (see Ref. [24] for an spectrum obtained at the Gran Sasso Laboratory), the recoil spectrum at the detector will turn out to be little sensitive to the exact form of the input neutron spectrum (see Table 3 and Fig. 8).

The transport of this neutron flux produced by fission or (α , n) reactions has been simulated in the IGEX geometries corresponding to the experimental

sets A, B and C (0, 20 and 40 cm of neutron moderator in the outer part of the shielding). The integrated rate seen by the Ge detector in the energy region from 4 to 10 keV for each case is listed in Table 3.

Table 3

Relative importance of neutrons coming from the radioactivity of the rock: calculated background rates for the different set-ups [expressed in counts/(keV kg day)] in the energy region from 4 to 10 keV assuming, either that all of them have a fission spectrum (second column), or that they come from (α, n) reactions (third column). A normalization of the input neutron flux of $3.82 \times 10^{-6} \text{ cm}^{-2} \text{ s}^{-1}$ has been assumed (see text).

	cm of moderator	fission	(α, n) reactions
A	0	6×10^{-1}	6×10^{-1}
B	20	5×10^{-3}	1×10^{-2}
C	40	$\sim 8 \times 10^{-5}$	$\sim 1 \times 10^{-4}$

Monte Carlo simulations of the propagation of neutrons through typical shieldings show that 90% of neutrons of 1 MeV (5 MeV) moderate down to $E < 0.1 \text{ eV}$ after 12 cm (22 cm) of polyethylene, and, in a shielding of 40 cm of polyethylene, 99.7% of neutrons of 5 MeV are moderated down to 0.1 eV (and practically all neutrons of 1 MeV). For neutrons of higher energies the fraction which is moderated down to $E < 0.1 \text{ eV}$ after, say, 40 cm of water is $\sim 92\%$ (for neutrons of 10 MeV), $\sim 83\%$ (for neutrons of 25 MeV) and $\sim 50\%$ (for neutrons of 50 MeV). Therefore one can assume that, given the energies of neutrons coming from radioactivity, 40 cm of polyethylene (or water) are enough to moderate their whole population. This is indeed what Table 3 shows: with 40 cm of moderator the neutron events are reduced by 3 or 4 orders of magnitude.

This fact can be used to find out the normalization of the input neutron flux. The simulation in case A (no moderator) can be directly compared with the spectrum obtained by subtraction of the experimental spectra C (40 cm of moderator) from A, under the assumption that the 40 cm polyethylene stops only neutrons coming from radioactivity. This is not strictly true, but it is a reasonable assumption taking into account the different magnitude of the flux of neutrons from radioactivity and the muon-induced neutron flux, as seen in the previous sections. In Fig. 8 the difference between the experimentally obtained spectra C and A is plotted together with the simulated fission and (α, n) neutron spectra, all three curves showing a remarkable agreement in their spectral shapes. The normalization of the simulation is fixed by minimizing the difference between simulated and experimental spectra, and it turns to be virtually the same for neutrons coming from fission or (α, n) . The fast neutron flux from radioactivity in the Canfranc rock is then deduced to be

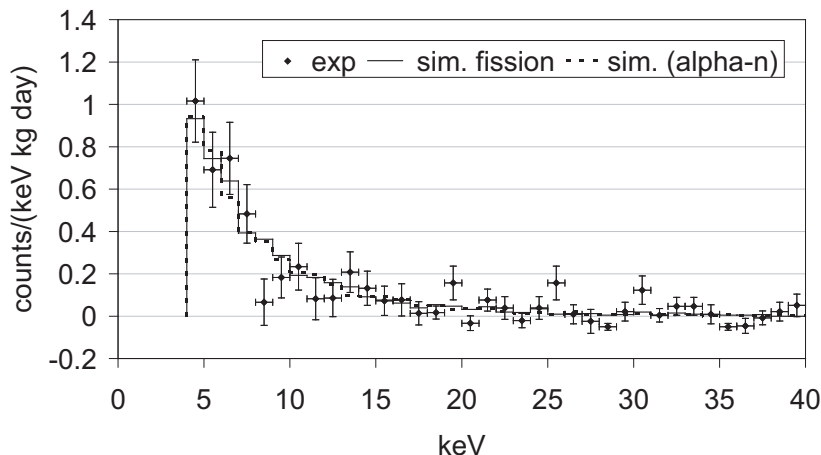


Fig. 8. Comparison of the simulated spectra of electron-equivalent energy deposited in the detector due to fission and (α, n) processes in the rock assuming no neutron moderator shielding (labelled *sim. fission* and *sim. (alpha-n)* respectively) with the difference between measured spectra for sets A and C (labelled *exp*).

$(3.82 \pm 0.44) \times 10^{-6} \text{ cm}^{-2} \text{ s}^{-1}$ which is within the expected range. Only statistical errors are quoted; the difference in the estimated flux when considering that all the neutrons have either the fission spectrum or that corresponding to (α, n) processes is less than 2%. The error due to the presence of muon-induced neutrons in the rock is estimated to be 0.04%, taking into consideration the simulated contribution of these neutrons to the counting rate of the experiment. We observe in Table 3 that for sets B and C, having 20 and 40 cm of neutron moderator, the contribution of (α, n) reaction neutrons is slightly higher than that of fission neutrons assuming the same flux for both.

As a conclusion for the understanding of the IGEX-DM background, it seems clear that this neutron flux is shielded by 40 cm of neutron moderator at our present level of sensitivity. In fact the neutron flux is almost eliminated with just 20 cm of moderator. This agrees with the experimental background shown in Table 1 for the set-up B where there was a lack of two moderator walls owing to the presence of dewars.

6 Conclusions

A complete quantitative study of the neutron environment in the LSC has been performed. The analysis is focused on the IGEX Dark Matter experiment, whose low energy raw background (with no nuclear recoil discrimination) is the lowest ever achieved. The study has consisted in a set of simulations compared with several sets of experimental data taken with the IGEX detector in dif-

ferent conditions of neutron shielding. In decreasing order of importance, the neutron populations studied, whose estimated fluxes are summarized in Table 4, are: neutrons coming from radioactivity in the laboratory rock, neutrons induced by muons in the lead shielding, and neutrons induced by muons in the laboratory rock. Neutrons produced by radioactivity in the lead shielding have been excluded from the analysis since they are negligible at the present level of background of IGEX-DM.

For neutrons produced by the interaction of muons in the lead of the shielding, the results of the simulations have been compared with the experimental spectrum obtained in coincidence with the vetoes, which has allowed to set the rate of production of these neutrons in lead at the LSC depth at $(4.8 \pm 0.6(stat) \pm 1.9(syst)) \times 10^{-9} \text{ cm}^{-3} \text{ s}^{-1}$ leading to a muon flux of $(2.47 \pm 0.31(stat) \pm 0.98(syst)) \times 10^{-7} \text{ cm}^{-2} \text{ s}^{-1}$. This number is in the range of the expected muon flux at that depth, and is in perfect agreement with previous measurements at the Canfranc site giving a flux of $2 \times 10^{-7} \text{ cm}^{-2} \text{ s}^{-1}$. The effect of these neutrons in the experimental data is small thanks to the muon veto system used [otherwise, this kind of events would contribute to 0.16 counts/(keV kg day) in the 4-10 keV region]. Improvements in the efficiency of the muon veto system might be necessary to reduce the effect of these neutrons in more sensitive experiments.

Regarding the neutrons coming from radioactivity in the rock, the simulations have been compared with experimental data taken with different thicknesses of neutron moderator, which has allowed us to set the flux of this kind of neutrons to $(3.82 \pm 0.44) \times 10^{-6} \text{ cm}^{-2} \text{ s}^{-1}$. We have concluded that the recent improvement reported in our article [7] is compatible with the complete rejection of this kind of neutrons that previously (in [6]) accounted up to 50% of the low energy data. With 40 cm of neutron moderator, these neutrons should contribute to the experimental data in less than 10^{-4} counts/(keV kg day).

Finally, with respect to the muon-induced neutrons in the rock, they have been simulated consistently with the previous information. From the incoming flux of muons, a flux of high energy neutrons going out of the rock of $(1.73 \pm 0.22(stat) \pm 0.69(syst)) \times 10^{-9} \text{ cm}^{-2} \text{ s}^{-1}$ is obtained, which finally contribute up to 10^{-4} counts/(keV kg day) to the IGEX-DM background, a number much below the present experimental level.

Briefly, the neutrons can be rejected as responsible for the low energy events that populate the last IGEX-DM data below ~ 20 keV substantially over the expectations (see [7]) and whose identification was partially the motivation of the present work. The information gathered by the present analysis will be also extremely useful in the design of future experiments in the LSC.

Table 4

Results for the estimates of the fluxes of different neutron populations reaching the IGEX-DM experimental setup in the LSC.

neutrons from radioactivity of the rock	$(3.82 \pm 0.44) \times 10^{-6} \text{ cm}^{-2} \text{ s}^{-1}$
muon-induced neutrons in the rock	$(1.73 \pm 0.22(\text{stat}) \pm 0.69(\text{syst})) \times 10^{-9} \text{ cm}^{-2} \text{ s}^{-1}$
muon-induced neutrons in the shielding lead	$(4.8 \pm 0.6(\text{stat}) \pm 1.9(\text{syst})) \times 10^{-9} \text{ cm}^{-3} \text{ s}^{-1}$

7 Acknowledgments

During the writing of this article, Prof. Angel Morales passed away. Even if it is impossible to express here how all of us are indebted to him, we wish to show our deepest and grateful acknowledgement not only for encouraging this study but also for sharing with us his knowledge and enthusiasm for work.

The Canfranc Underground Laboratory is operated by the University of Zaragoza. This research was partially funded by the Spanish Ministry of Science and Technology (MCYT) under contract No. FPA2001-2437. We are indebted to our IGEX colleagues for their collaboration in the IGEX and IGEX-DM experiments.

References

- [1] D.N. Spergel *et al.*, *Astrop. Phys. J. Suppl.* 148 (2003) 175. See recent results of MAP on <http://map.gsfc.nasa.gov/>.
- [2] R.A. Knop *et al.*, *Astrop. Phys. J.* 598 (2003) 102. See recent results of SN project on <http://panisse.lbl.gov/>.
- [3] M. Tegmark *et al.*, *astro-ph/0310723* (accepted in *Phys. Rev. D*). See recent results of SDSS on <http://www.sdss.org/>.
- [4] A. Morales, Review Talk at the XXXth International Winter Meeting on Fundamental Physics, Jaca, Huesca (Spain), 2002, *Nucl. Phys. B (Proc. Suppl.)* 114 (2003) 39; A. Morales, Review Talk at the TAUP2003, Seattle (USA), to appear in the Proceedings.
- [5] A. da Silva *et al.*, *NIM A* 354 (1995) 553.
- [6] A. Morales *et al.* [IGEX Collaboration], *Phys. Lett. B* 489 (2000) 268.
- [7] A. Morales *et al.* [IGEX Collaboration], *Phys. Lett. B* 532 (2002) 8.
- [8] I.G. Irastorza *et al.*, *Astrop. Phys.* 20 (2003) 247.

- [9] R. Abusaidi *et al.* [CDMS Collaboration], Phys. Rev. Lett. 84 (2000) 5699; D. Abrams *et al.* [CDMS Collaboration], Phys. Rev. D 66 (2002) 122003; D. Akerib *et al.* [CDMS Collaboration], Phys. Rev. D 68 (2003) 082002.
- [10] A. Benoit *et al.* [EDELWEISS Collaboration], Phys. Lett. B 513 (2001) 15; A. Benoit *et al.* [EDELWEISS Collaboration], Phys. Lett. B 545 (2002) 43.
- [11] M. Bravin *et al.* [CRESST Collaboration], NIM A 444 (2000) 323; G. Angloher *et al.* [CRESST Collaboration], Astrop. Phys. 18 (2002) 43.
- [12] S. Cebrián *et al.*, Phys. Lett. B 563 (2003) 48.
- [13] G. Chardin, Proceedings of the Fourth International Workshop on Identification of Dark Matter 2002, York (England), World Scientific p. 470.
- [14] H. Wulandari, Proceedings of the Fourth International Workshop on Identification of Dark Matter 2002, York (England), World Scientific p. 464; H. Wulandari *et al.*, hep-ex/0401032.
- [15] V.A. Kudryavtsev, N.J.C. Spooner, and J.E. McMillan, NIM A 505 (2003) 683; V. A. Kudryavtsev, Proceedings of the Fourth International Workshop on Identification of Dark Matter 2002, York (England), World Scientific p. 477.
- [16] T.A. Perera, PhD thesis, Case Western Reserve University (2002).
http://cosmology.berkeley.edu/preprints/cdms/Dissertations/tap_thesis.pdf
- [17] C.E. Aalseth *et al.*, Phys. Rev. C 59 (1999) 2108; D. González *et al.*, Nucl. Phys. B (Proc. Suppl.) 87 (2000) 278; C.E. Aalseth *et al.*, Phys. Rev. D 65 (2002) 092007.
- [18] G. Heusser, Ann. Rev. Nucl. Part. Sci. 45 (1995) 543.
- [19] S. Agostinelli *et al.* [GEANT4 Collaboration], NIM A 506 (2003) 250.
- [20] A. Fassò, A. Ferrari, P.R. Sala, “Electron-photon transport in FLUKA: status”, Proceedings of the MonteCarlo 2000 Conference, Lisbon, October 23–26 2000, A. Kling, F. Barao, M. Nakagawa, L. Tavora, P. Vaz eds., Springer-Verlag Berlin, p. 159-164 (2001); A. Fassò, A. Ferrari, J. Ranft, P.R. Sala, “FLUKA: Status and Prospective for Hadronic Applications”, *ibid*, p. 955-960 (2001).
- [21] S.R. Golwala, PhD thesis, University of California at Berkeley (2000).
<http://cosmology.berkeley.edu/preprints/cdms/golwalathesis/>
- [22] P. Lipari *et al.*, Phys. Rev. D 44 (1991) 3543.
- [23] F.F. Khalchukov *et al.*, Il Nuovo Cimento 6C (1983) 320; F.F. Khalchukov *et al.*, Il Nuovo Cimento 18C (1995) 517.
- [24] H. Wulandari *et al.*, hep-ex/0312050.
- [25] P. Belli *et al.*, Il Nuovo Cimento A 101 (1989) 959.
- [26] A. Rindi *et al.*, NIM A 272 (1988) 871.
- [27] V. Chazal *et al.*, Astrop. Phys. 9 (1998) 163.

- [28] J.N. Abdurashitov *et al.*, Nucl. Phys. B (Proc. Suppl.) 110 (2002) 320.
- [29] H.J. Kim *et al.*, Astrop. Phys. 20 (2004) 549.
- [30] S.R. Hashemi-Nezhad, L.S. Peak, NIM A 357 (1995) 524.